THE JOURNAL OF PHYSICAL CHEMISTRY B

Article

pubs.acs.org/JPCB

Coordination Number of Li^+ in Nonaqueous Electrolyte Solutions Determined by Molecular Rotational Measurements

Kaijun Yuan,[†,‡] Hongtao Bian,[‡] Yuneng Shen,[†] Bo Jiang,[†] Jiebo Li,[‡] Yufan Zhang,[‡] Hailong Chen,[‡] and Junrong Zheng*[,‡]

[†]State key Laboratory of Molecular Reaction Dynamics, Dalian Institute of Chemical Physics, Chinese Academy of Sciences, 457 Zhongshan Road, Dalian 116023, China

[‡]Department of Chemistry, Rice University, Houston, Texas 77005, United States

Supporting Information

ABSTRACT: The coordination number of Li^+ in acetonitrile solutions was determined by directly measuring the rotational times of solvent molecules bound and unbound to it. The CN stretch of the Li^+ bound and unbound acetonitrile molecules in the same solution has distinct vibrational frequencies (2276 cm^{-1} vs 2254 cm^{-1}). The frequency difference allows the rotation of each type of acetonitrile molecule to be determined by monitoring the anisotropy decay of each CN stretch vibrational excitation signal. Regardless of the nature of anions and concentrations, the Li^+ coordination number was found to be 4−6 in the $LiBF_4$ (0.2−2 M) and $LiPF_6$ (1−2 M) acetonitrile solutions. However, the dissociation constants of the salt are dependent on the nature of anions. In 1 M $LiBF_4$ solution, 53% of the salt was found to dissociate into Li^+, which is bound by 4−6 solvent molecules. In 1 M $LiPF_6$ solution, 72% of the salt dissociates. 2D IR experiments show that the binding between Li^+ and acetonitrile is very strong. The lifetime of the complex is much longer than 19 ps.

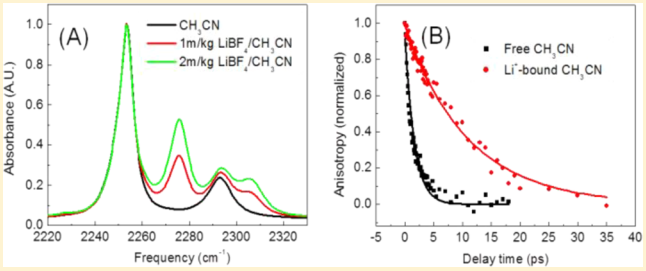

1. INTRODUCTION

Batteries based on the Li^+ cation have been powering our daily digital life for many years. The state-of-the-art of Li^+ ion batteries are composed of two electrodes that contain intercalation materials to host Li^+ and between which there is a layer of nonaqueous electrolyte solution to conduct ions.[1,2] The solute of the electrolyte solution is typically a lithium salt, e.g., $LiPF_6$, dissolved in a mixture of carbonate organic solvents. The basic function of the electrolyte solution is to transport Li^+ cations and anions, which determines how fast the energy stored on electrodes can be delivered.[3] It is widely believed that the transport of ions in the solution is a two-stepped process: (1) the solvation of ions by the solvent molecules and (2) the migration of the solvated ions. The ionic conductivity that quantifies the ion conduction ability in a solution is the overall result of these two steps. Therefore, to design new materials to improve the conductivity of Li^+, knowledge about how Li^+ is solvated by solvent molecules is indispensable. In addition, recent research also suggests that the formation and chemical composition of the solid electrolyte interphase (SEI) on the anode surface, which is critical for the stabilization of the electrolyte/anode interface, are dictated by the Li^+ solvation sheath.[4,5]

The importance of Li^+ solvation has drawn many research efforts from both theory and experiments to understand how Li^+ interacts with organic solvent molecules.[6] Ab initio calculations suggest that the small ionic radius of lithium generally does not allow more than five organic solvent molecules to directly bind to it.[7] Mass spectrometry and NMR measurements seem to support the calculated results.[8,9] Recent XRD experiments[10,11] suggest that a Li^+ cation is fully solvated by four directly bound and two uncoordinated acetonitrile molecules in a crystal. The most recent NMR experiments suggest that maximum six ethylene carbonate molecules can coexist in the Li^+ solvation sheath.[4] All these previous experiments have provided very important information for the understanding of Li^+ solvation, but most of the measurements either are indirect for the determination of the coordinate number (e.g., from chemical shifts) or are under conditions that are not close enough to the actual environments of applications (e.g., crystals in XRD measurements and molecules in gas phase in MS measurements).

Different from those traditional methods, here we present an approach for the direct determination of Li^+ coordination number in nonaqueous electrolyte solutions. The method is based on directly measuring molecular rotational times in solutions. It is to respectively measure the rotational time constants of free and Li^+-bound solvent molecules in the same or different solutions by monitoring the real time anisotropy decay of the vibrational excitation signal of a vibration band of the solvent molecule. The coordination number of Li^+ can then be straightforwardly obtained from comparison between the

Received: January 24, 2014
Revised: March 12, 2014
Published: March 14, 2014

   dx.doi.org/10.1021/jp500877u | J. Phys. Chem. B 2014, 118, 3689−3695

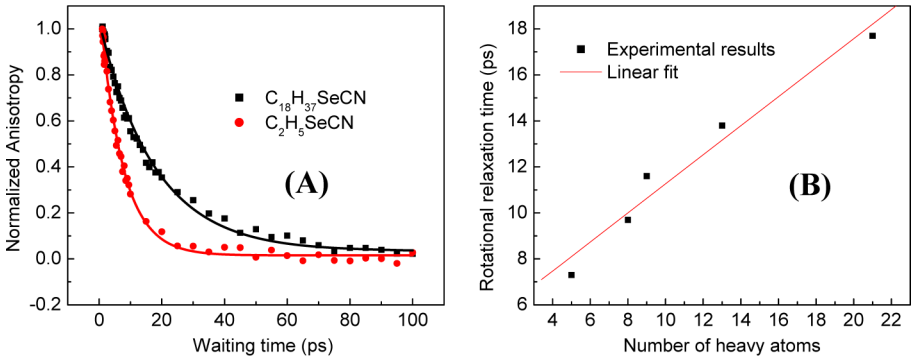

Figure 1. (A) Anisotropy decay curves of the nitrile stretch excitation signal (from the ground state to the first excited state) of C_2H_5SeCN and $C_{18}H_{37}SeCN$ in dilute CCl_4 solutions (3.5 wt %). (B) Correlation between the rotational time constants from the analyses of the anisotropy decay curves with single exponential and the number of heavy atoms of $CH_3-(CH_2)_n-SeCN$ molecules.

rotational time constants of free and Li^+-bound solvent molecules, following the Stokes–Einstein equation, which states that the rotational diffusion time constant is proportional to the volume of the rotor (molecule):[12]

$$D_r = \frac{kT}{8\pi\eta r^3} \quad (1)$$

where D_r is the rotational diffusion time constant, η is the viscosity, r is the particle radius, T is temperature, and k is the Boltzmann constant. The general applicability of the Stokes–Einstein equation to molecular rotations in organic solutions is tested with two molecular systems. Figure 1A displays the anisotropy decay curves of the nitrile stretch excitation signal (from the ground state to the first excited state) of C_2H_5SeCN and $C_{18}H_{37}SeCN$ in dilute CCl_4 solutions (3.5 wt %), and Figure 1B displays the correlation between the rotational time constants from the analyses of the anisotropy decay curves with single exponential and the number of heavy atoms of which the mass is heavier than that of H of $CH_3-(CH_2)_n-SeCN$ molecules (Supporting Information, Table S1). The data clearly show that the rotational time constant becomes longer for a larger molecule. To more quantitatively explore the correlation between molecular rotational volume and time, the vibrational excitation signal anisotropy decays of $HO-C_6H_4-CN$ and $HO-C_6H_4-C_6H_4-CN$ were also measured (Supporting Information, Figure S1). The volume of $HO-C_6H_4-C_6H_4-CN$ is estimated to be about 100% larger than that of $HO-C_6H_4-CN$ as it has one more benzene ring compared to which the volumes of OH and CN are very small. The rotational time constant of $HO-C_6H_4-CN$ is 18 ± 2 ps, and that of $HO-C_6H_4-C_6H_4-CN$ is 40 ± 4 ps. The ratio of the rotational time constants is essentially the same as the volume ratio of these two molecules. The two examples show that the Stokes–Einstein equation works reasonably well for simple molecular systems in organic solutions.

In this work, we applied the method to determine the Li^+ coordination number in the solutions of lithium salts dissolved in acetonitrile (CH_3CN).

2. EXPERIMENTS AND MATERIALS

The laser setup is similar to that described previously.[13] A picosecond amplifier and a femtosecond amplifier are synchronized with the same oscillator. The picosecond amplifier pumps an OPA to produce ~1.4 ps (vary from 1.3 to 1.5 ps in different frequencies) mid-IR pulses with a bandwidth ~15 cm^{-1} in a tunable frequency range from 400 to 4000 cm^{-1} with energy 1–40 μJ/pulse (1–10 μJ/pulse for 400–900 cm^{-1} and >10 μJ/pulse for higher frequencies) at 1 kHz. Light from the femtosecond amplifier is used to generate a high-intensity mid-IR and terahertz supercontinuum pulse. A collimated 800 nm beam from the femtosecond amplifier is frequency doubled by passing through a Type-I 150 μm thick BBO crystal cut at 29.2° to generate 400 nm light. A dual waveplate is used to tune the relative polarizations of the 800 and 400 nm pulses, which functions as a full-wave plate at 400 nm and a half-wave plate at 800 nm. Temporal delay between two beams is compensated by inserting a 2 mm thick BBO (cut at 55°) between the doubling crystal and the wave plate, where the 800 and 400 nm pulses propagate with orthogonal polarizations with different velocities in the delay plate.[14−16] The supercontinuum pulse is then generated by focusing the two copropagating beams in air, with a pulse duration around 110 fs in the frequency range from <20 to >3200 cm^{-1} at 1 kHz, and the shot to shot fluctuation is less than 1% in the most of the spectral region. In nonlinear IR experiments, the picosecond IR pulse is the excitation beam (the excitation power is adjusted on the basis of need). The supercontinuum pulse is the detection beam which is frequency resolved by a spectrograph (resolution is 1–3 cm^{-1} dependent on the frequency) yielding the detection axis of a 2D IR spectrum. Scanning the excitation frequency yields the other axis of the spectrum. Two polarizers are inserted into the detection beam path to selectively measure the parallel or perpendicular polarized signal relative to the excitation beam. The entire setup including frequency and polarization tuning is computer controlled. Vibrational lifetimes are obtained from the rotation-free signal $P_{life} = P_{\parallel} + 2 \times P_{\perp}$, where $P_{\parallel}$ and $P_{\perp}$ are parallel and perpendicular data, respectively. Rotational relaxation dynamics are acquired from the time dependent anisotropy $R = (P_{\parallel} - P_{\perp})/(P_{\parallel} + 2 \times P_{\perp})$. The heat effects from vibrational relaxations were removed, following the procedure described in our previous publication:[17] the heat signal is assumed to grow with time constants slightly slower than the lifetimes of vibrational excitations generating heat. The maximum amplitude of the heat signal is the transient signal at very long waiting times after most vibrational excitations have relaxed. The time dependent heat signal calculated in this way is subtracted from the transient signal (for both $P_{\parallel}$ and $P_{\perp}$).

Chemicals were purchased from Aldrich and Cambridge Isotope and used as received. The synthesis of $CH_3(CH_2)_nSeCN$ follows the literature:[18] potassium selenocyanate (KSeCN, 288 mg, 2 mmol) and DMF (30 mL) are

dx.doi.org/10.1021/jp500877u | J. Phys. Chem. B 2014, 118, 3689–3695

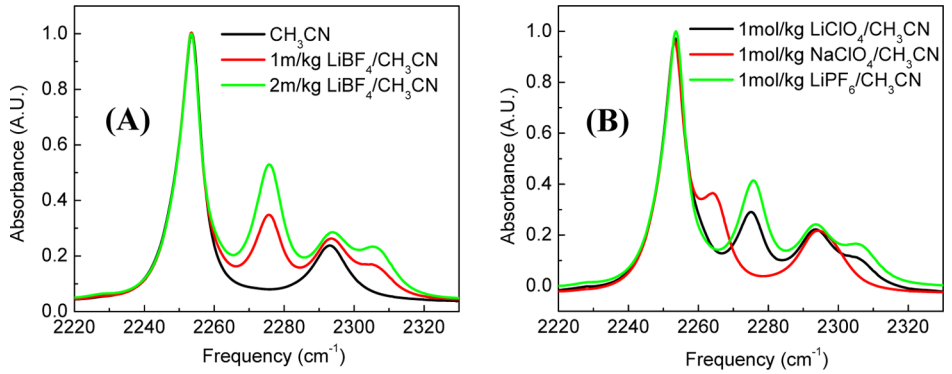

Figure 2. FTIR spectra of (A) CH_3CN, 1 mol/kg $LiBF_4/CH_3CN$, 2 mol/kg $LiBF_4/CH_3CN$, and (B) 1 mol/kg $LiClO_4/CH_3CN$, 1 mol/kg $NaClO_4/CH_3CN$, and 1 mol/kg $LiPF_6/CH_3CN$.

mixed in a 250 mL three-necked flask under an argon shield. *n*-Decyl bromide (450 μL in 10 mL DMF) is introduced by a isobaric funnel into the solution. The mixture is stirred at 20 °C for 26 h and then hydrolyzed with 30 mL of water and extracted twice with 50 mL of ether. The ethereal fractions are combined, washed with water (3 × 20 mL), and dried over $MgSO_4$. The solvent is evaporated in vacuum. The crude mixture is fractionated with column chromatography of silica gel using petroleum ether as fluent. The final product is collected in yellow oil. Lithium salts were dried in the vacuum oven with P_2O_5, and the solutions were prepared in a glovebox. The liquid samples in the FTIR and 2D IR measurements were contained in a sample cell composed of two CaF_2 windows separated by a Teflon spacer. The thickness of the spacer was adjusted on the basis of the optical densities. The samples were assembled in glovebox and glove bags. The experimental optical path and apparatus were purged with clean air free of CO_2 or water. Unless specified, all measurements were carried out at room temperature (297 K). Viscosities were measured with a Cannon–Fenske kinematic viscosity tube.

Density functional theory (DFT) calculations were carried out using Gaussian 09. The level and basis set used were Becke's three-parameter hybrid functional combined with the Lee–Yang–Parr correction functional, abbreviated as B3LYP, and 6-311++G(d,p).

3. RESULTS AND DISCUSSION

3.1. Li^+ Binding Blue Shifts the Vibrational Frequency of the CN Stretch. Figure 2A displays the FTIR spectra of CH_3CN, 1 mol/kg $LiBF_4/CH_3CN$, 2 mol/kg $LiBF_4/CH_3CN$ in the CN stretch frequency region. In the pure CH_3CN (black curve), based on DFT calculations and previous experimental results,[19] the main peak at ~2254 cm^{-1} is assigned to the CN stretch, and the small peak at ~2294 cm^{-1} is assigned to a combination band. With the addition of $LiBF_4$, a peak at ~2276 cm^{-1} and a small shoulder at ~2306 cm^{-1} grow in. The two peaks grow in with the increase of $LiBF_4$ concentration. The results indicate that the two small peaks are caused by the binding of either Li^+ or BF_4^- to CH_3CN. To further investigate which ion causes the frequency blue shifts, FTIR spectra of 1 mol/kg $LiClO_4/CH_3CN$, 1 mol/kg $NaClO_4/CH_3CN$, and 1 mol/kg $LiPF_6/CH_3CN$ were collected and displayed in Figure 2B. Changing the anions from BF_4^- (Figure 2A) to ClO_4^- (Figure 2B black curve) or PF_6^- (Figure 2B green curve) does not change the frequencies of these two small peaks. However, the small peaks in the Li^+ solutions obviously red shift from ~2276 to ~2264 cm^{-1} when Li^+ is replaced by Na^+ (Figure 2B red curve). The results suggest that the peak at ~2276 cm^{-1} and the small shoulder at ~2306 cm^{-1} in the Li^+ solutions are caused by the binding of Li^+ to CH_3CN.

The next question is which CH_3CN molecules produce these two small peaks: (1) those directly bind to Li^+ or (2) those within the first few solvation shells of Li^+. This question is difficult to be experimentally answered, but we can perform DFT calculations to explore it. For a $Li^+\cdots NCCH_3$ complex, the calculated Li–N distance is 1.89 Å, and the calculated vibrational frequency of CN stretch is 2264 cm^{-1} (scaling factor 0.954), 10 cm^{-1} larger than that of the free CH_3CN (2254 cm^{-1}). For a CH_3CN that is in the second solvation shell of Li^+, the shortest Li–N distance is ~4.5 Å. We calculated the vibrational frequency of CN stretch for two Li–N distances: 4 and 8 Å. Both calculations give the same frequency: 2252 cm^{-1}. The calculations indicate that only the CH_3CN molecules in the first solvation shell of Li^+ that directly bind to Li^+ can blue shift the frequency of the CN stretch. On the basis of the experimental and theoretical results, we can assign the peak at 2276 cm^{-1} to the CN stretch of CH_3CN which is directly bound to Li^+.

3.2. CH_3CN Rotates 1.3 ps in Acetonitrile Liquids. In liquids at room temperature, because of collisions, molecules can rotate very fast at the picosecond (10^{-12} second) time scale. The fast rotational motions can be monitored in real time by tracing the anisotropy decay of the excitational signal of a certain vibrational mode of the molecule with ultrafast infrared laser pulses, in a way similar to that of anisotropy measurement with time-resolved fluorescence.[20] In general, the anisotropy decay of vibrational excitation has three origins.[20,21] One is the molecular rotation. Another is the resonant energy transfer from the energy donor to a randomly oriented acceptor. The third one is the two-stepped nonresonant energy transfers from one energy donor to a nonresonant energy acceptor and then from this acceptor to another molecule of the same type of the original energy donor but with a different orientation. For most small molecules of which rotational times are only a few picoseconds in liquids, the third contribution to anisotropy decay is relatively small, because it takes a long time for the two-stepped nonresonant energy transfer to occur, which is typically slower than tens or hundreds of picoseconds.[22] In pure liquids[23,24] or concentrated solutions,[25] resonant vibrational energy transfers can be comparable to or faster than molecular rotations and make a significant contribution to the experimentally observed anisotropy decay. For these cases, one needs to independently measure the resonant energy

dx.doi.org/10.1021/jp500877u | J. Phys. Chem. B 2014, 118, 3689–3695

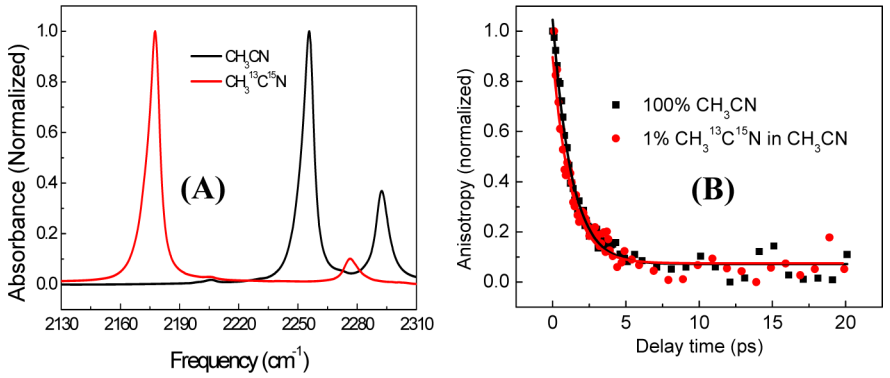

Figure 3. (A) FTIR spectra of CH_3CN and $CH_3{}^{13}C^{15}N$ and (B) anisotropy decay curves of the nitrile stretch vibrational excitation signal of CH_3CN in pure CH_3CN and $CH_3{}^{13}C^{15}N$ in $CH_3CN/CH_3{}^{13}C^{15}N$ = 99/1. Dots are data, and the curves are fits of a single exponential with a time constant ~1.3 ps.

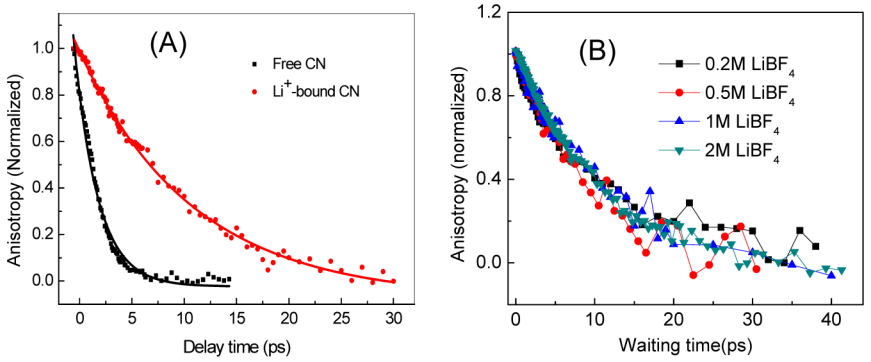

Figure 4. (A) Time dependent anisotropies of nitrile stretch of free CH_3CN and Li^+-bound CH_3CN in a 1 mol/kg $LiBF_4/CH_3CN$ solution. (B) Time dependent anisotropies of nitrile stretch of Li^+-bound CH_3CN of 0.2−2 mol/kg $LiBF_4/CH_3CN$ solutions.

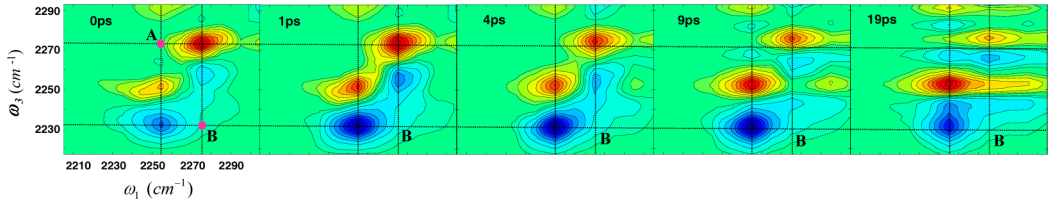

Figure 5. Waiting time dependent 2D IR spectra of $LiBF_4/CH_3CN$ 1 mol/kg solution.

transfer rate or suppress the resonant energy transfer by diluting the liquid with isotope labeled species to obtain the molecular rotational time from the anisotropy decay measurement.

The liquids studied in this work are pure CH_3CN and their lithium salt solutions. In these liquids, it is conceivable that resonant vibrational energy transfers among the organic molecules can occur at a fast time scale comparable to that of the molecular rotations. Therefore, to obtain the rotational time constant of CH_3CN in the pure acetonitrile, we respectively measured the anisotropy decay of the nitrile stretch vibrational excitational signal of CH_3CN in the pure CH_3CN and $CH_3{}^{13}C^{15}N$ in a $CH_3CN/CH_3{}^{13}C^{15}N$ = 99/1 mixture, as displayed in Figure 3B. Isotope labeled $CH_3{}^{13}C^{15}N$ has a nitrile stretch frequency at 2177 cm^{-1}, 77 cm^{-1} lower than that of CH_3CN (Figure 3A). Estimated from the vibrational energy transfer equation from our previous studies on liquid samples,[22] the frequency shift of 77 cm^{-1} causes the energy transfer from the nitrile stretch of CH_3CN to that of $CH_3{}^{13}C^{15}N$ about 20 times slower than the resonant energy transfer between two CH_3CN. If resonant energy transfers among CH_3CN contribute significantly to the anisotropy decay in the pure liquid (black dots), we would expect to see that the anisotropy decays should be much slower in the $CH_3CN/CH_3{}^{13}C^{15}N$ = 99/1 (red dots) mixtures because the resonant energy transfers among the same type of nitrile stretch are significantly suppressed by the dilution of isotope labeled species which does not change the molecular rotational dynamics (according to the Stokes−Einstein equation). Experimentally, in both liquids the anisotropy decays are essentially the same within experimental uncertainty, indicating that the energy transfers in the liquids are much slower than the molecular rotations. Therefore, the anisotropy decay time constant 1.3 ± 0.2 ps from the three measurements can be considered as the CH_3CN (or $CH_3{}^{13}C^{15}N$) rotational time constant in the liquids.

3.3. Li^+-Bound CH_3CN Rotates ~4.8 Times Slower Than Unbound CH_3CN in 1 M $LiBF_4$/Acetonitrile Solutions. Figure 4A displays the time dependent anisotropies of the nitrile stretch of free CH_3CN (excited at 2254 cm^{-1}) and Li^+-bound CH_3CN (excited at 2276 cm^{-1}) in a 1 mol/kg

dx.doi.org/10.1021/jp500877u | J. Phys. Chem. B 2014, 118, 3689−3695

$LiBF_4/CH_3CN$ solution. The anisotropy decay of the Li^+-bound CH_3CN is much slower than that of free CH_3CN. The decay time constant of the Li^+-bound CH_3CN is 11 ± 1 ps, which is about 4.8 times of that (2.3 ± 0.2 ps) of the free CH_3CN. As discussed above, because the energy transfers in the CH_3CN are much slower than that of the molecular rotation, the anisotropy time ratio can be considered as the rotational time ratio between the Li^+-bound and unbound species. The very likely reason for the much slower rotation of the Li^+-bound species is that several CH_3CN molecules are bound by one Li^+ so that the whole complex of which the volume is much larger than that of a single CH_3CN rotates together.

3.4. Li^+/CH_3CN Complex Lasts Much Longer Than 19 ps. This above assumption that the Li^+ cation and CH_3CN molecules bound to it rotate together for 11 ps is supported by the 2D IR measurements on a 1 mol/kg $LiBF_4$/acetonitrile solution in Figure 5, which shows that up to 19 ps no chemical exchange peaks between the Li^+-bound and unbound species have grown in, indicating that the Li^+-bound molecules can stay together for much longer than 19 ps.

The chemical exchange 2D IR spectra and methods have been previously elaborated.[26−29] Here only a brief description is provided. In Figure 5, the red peak at ∼2276 cm^{-1} and the blue peak below it along *y*-axis are the 0−1 and 1−2 transition peaks of the CN stretch of the Li^+-bound CH_3CN. The red peak at ∼2254 cm^{-1} and the blue peak below it along *y*-axis are the 0−1 and 1−2 transition peaks of the CN stretch of the free CH_3CN. If the Li^+-bound CH_3CN can dissociate into free CH_3CN after a certain reaction time, the dissociation must produce a blue cross peak at the position of B (the cross point of two lines) at long waiting times, e.g., 19 ps. For the same reason, the binding between a free CH_3CN with a Li^+ to form a Li^+-bound CH_3CN must produce a red cross peak at the position of A at long waiting times. However, as shown in Figure 5, even up to 19 ps, no blue cross peak at position B grows, indicating that no Li^+-bound CH_3CN dissociation is detected. The result implies that the average lifetime of Li^+/CH_3CN complex must be much longer than 19 ps, according to the calculation of the chemical exchange kinetic model analyses.[30−33] According to chemical equilibrium, within 19 ps, no Li^+/CH_3CN association should be observed either. However, we do see a red cross peak above the line of $y = 2276$ cm^{-1} at 19 ps in Figure 5. This peak is not caused by the association of Li^+ and CH_3CN. This red peak and its blue peak and the cross peak pair above B in the 19 ps panel are caused by the vibrational relaxation induced bleaching and absorption,[34] similar to those in the mixture of CH_3CN/C_6H_5CN we elaborated before.[35] Other peaks with either *x*- or *y*-axis larger than 2276 cm^{-1} are caused by the energy transfers between the combination bands at the higher frequencies shown in Figure 2 and the CN stretches. The detailed analyses of coupling and energy transfer peaks between a normal mode and a combination band can be found in our previous publication.[36] The results show that up to 19 ps, no Li^+/CH_3CN association or dissociation has occurred for a noticeable amount. Although we are not able to measure the dissociation time of the Li^+/CH_3CN complex (limited by the vibrational lifetimes of the CN stretches) except its fast limit, we are still able to estimate that the formation enthalpy absolute value of the Li^+/CH_3CN complex must be larger than 3 kcal/mol from the fast limit of the dissociation time reflected from Figure 5 and our previous results on the correlation between the H-bond complex formation enthalpy and dissociation time constant.[27]

3.5. Li^+/CH_3CN Complex Rotates without Anions. It is conceivable that one or two anions could also attach to the Li^+-bound complex and the anions could rotate together with the Li^+/CH_3CN complex. If this is the case, the measured rotational time is the time of such a multiple-ion complex. This concern can be tested by measuring the concentration dependent anisotropy decay. In a more concentrated solution, the chance for the anions to combine to the complex must be larger and, if so, the rotation of the complex should be slower if the global viscosity effect is not taken into consideration.

Figure 4B shows the anisotropy decay curves of the Li^+-bound CH_3CN CN stretch excitation signal in 0.2−2 mol/kg $LiBF_4/CH_3CN$ solutions. They are very similar, giving time constants within the range 9.5 ± 1.5 ps. In the 0.2 M solution, the time constant is 9.5 ± 1.0 ps. The time constant is 10.0 ± 1.0 ps for the 0.5 M solution and 11.0 ± 1.0 ps for the 1 and 2 M solutions. It seems that the rotation becomes slightly slower in a more concentrated solution. However, within the experimental uncertainty all these rotational time constants are the same. In addition, in the 0.2 M solution, the $LiBF_4/CH_3CN$ molar ratio is about 1/122. We expect that in such a dilute solution, the chance for the cations and anions to form contact or one-solvent-separate ion pairs is very small because there is a sufficient number of solvent molecules to solvate both ions. Therefore, the anisotropy decay time 9.5 ± 1.0 ps in the 0.2 M solution can be considered as the rotational time constant of the Li^+-bound CH_3CN complex without any anions. We suspect that the slightly slower rotations in the more concentrated solutions are probably because of the global viscosity increase. The solution viscosity increases from ∼1.1 in the 0.2 M solution (relative value to that (taken as 1) of the pure CH_3CN, in Figure S7 (Supporting Information) to ∼2.3 in the 2 M solution. This explanation is supported by the fact that the rotation of the "free" CH_3CN molecules at 2254 cm^{-1} becomes slower in a more concentrated solution. The rotational time constants are 1.9 ± 0.2 ps (0.2 M), 2.0 ± 0.2 ps (0.5 M), 2.3 ± 0.2 ps (1 M), and 2.5 ± 0.2 ps (2 M). Detailed data are provided in the Supporting Information. The slowdown amplitude of the rotations of these "free" solvent molecules is much more obvious than that of the Li^+-bound species. This is explainable: as the concentration increases, the ions have more chances to form direct contact ion pairs or even clusters that are surrounded by the "free" species of which the CN frequency probably remains at 2254 cm^{-1} as the ion pairs of clusters are neutral or weakly charged. Such a situation can severely affect the rotations of these molecules but not those of Li^+-bound species.

Further experimental evidence to support that the measured 10 ps is the rotational time of complex not containing anions comes from the measurements on another lithium salt $LiPF_6$ which has a much larger anion and better ion dissociation ability. In the solutions of 1 mol/kg and 2 mol/kg $LiPF_6/CH_3CN$ solutions (Supporting Information, Figures S5 and S6), the rotational time constant (10 ± 1 ps) is similar to that of the $LiBF_4$ solutions, indicating the nature of anion does not have a detectible effect on the rotational dynamics of Li^+-bound complex.

3.6. One Li^+ Directly Binds to 4−6 CH_3CN. Summarizing all the experimental results presented above, the coordination number of Li^+ in acetonitrile should be very close to the rotational time ratio of the Li^+-bound CH_3CN over the "free"

dx.doi.org/10.1021/jp500877u | J. Phys. Chem. B 2014, 118, 3689−3695

CH_3CN in the same solution. A more dilute solution gives a more precise result as the effects of anions and ion pairs and clusters on the molecular rotations are smaller. The ratios in the $LiBF_4$ solutions are 5.0 (0.2 M), 5.0 (0.5 M), 4.8 (1 M), and 4.4 (2 M). The ratios in the $LiPF_6$ solutions are 5.1 (1 M) and 4.5 (2 M). Including the experimental uncertainty, all the experiments suggest that in the Li^+ salt acetonitrile solutions one Li^+ directly binds to 5.0 ± 1 CH_3CN molecules. If the volume associated with the binding of Li^+ is also considered, the actual coordination number of Li^+ is probably slightly smaller than 5. We therefore conclude that the coordination number of Li^+ in acetonitrile solutions at room temperature is 4−6. This value is the same as that obtained by ab initio calculations.[7]

3.7. $LiBF_4$ Dissociates Only ∼53% in the 1 mol/kg $LiBF_4/CH_3CN$ Solution. In the lithium salt acetonitrile solutions, the salt molecules cannot dissociate completely and many of them remain neutral as uncharged ion pairs or ion clusters, similar to what happens in aqueous solutions.[21,25,37] These neutral species do not move under applied electrical potential and do not contribute to the ion conductivity of the solution. A salt with better dissociation ability can provide more ions and thus better conductivity in a solution. It is therefore important to explore how many of the $LiBF_4$ molecules can dissociate ($LiBF_4 \rightarrow Li^+ + BF_4^-$) in the solutions. We are able to calculate the percentage of dissociated $LiBF_4$ in the 1 mol/kg solution in the following way. In the solution, the molar ratio of $CH_3CN/LiBF_4$ is 24.4. The molar ratio of the Li^+-bound/free CH_3CN is determined by the peak area ratio of peak-2276-cm^{-1}/peak-2254-cm^{-1} in the FTIR spectrum normalized with the square of transition dipole moments of these two species. The transition dipole moment square ratio of the Li^+-bound and free CH_3CN can be determined from both FTIR and pump/probe or 2D IR measurements, following the method described in our previous publication,[24,29] which is based on the fact the FTIR signal $I_{FTIR} = k_1 C\mu^2$ and the pump/probe or 2D IR signal $I_{3rd\ order} = k_2 C\mu^4$, where k_1 and k_2 are constants, C is the concentration, and μ is the transition dipole moment. The determined CN stretch transition dipole moment square ratio of Li^+-bound/free CH_3CN is 2.4 for both $LiBF_4$ and $LiPF_6$ solutions. Therefore, based on this ratio and the peak area ratio from FTIR spectrum, the Li^+-bound/free acetonitrile number ratio is 0.122/1. Here we assume that the undissociated $LiBF_4$ molecules do not change the vibrational frequency of the nitrile stretch of acetonitrile. This assumption is probably valid, because as we can see from Figure 2B Na^+ (red curve) only slightly shifts the CN stretch frequency. Compared to the charge density of Li^+, that of Na^+ is smaller because of its larger radius, and therefore its ability to change the CN stretch frequency is smaller. The charge density of $Li^+BF_4^-$ pair is considered to be much smaller than that of Na^+ because it is essentially a neutral species. Because of this, we expect that the $Li^+BF_4^-$ pairs or $(Li^+BF_4^-)_n$ clusters have very little effect on the CN stretch frequency. On the basis of the determined Li^+ coordination number −5, the dissociation percentage of $LiBF_4$ is calculated to be $24.4 \times (0.122)/(1.122) \times 1/(4.8) = 53\%$. In other words, 53% of $LiBF_4$ has dissociated into Li^+, which is fully solvated by CH_3CN (no BF_4^- is in the Li^+ first solvation shell) in the 1 mol/kg $LiBF_4$ acetonitrile solution. Following the same procedure, the dissociation percentage of $LiBF_4$ in the 2 mol/kg $LiBF_4$ acetonitrile solution is determined to be 42%, smaller than that in the 1 mol/kg solution, resulting from that fewer acetonitrile molecules are available to solvate Li^+ in the 2 mol/kg solution. The dissociation percentage of $LiPF_6$ in 1 mol/kg $LiPF_6$ acetonitrile solution is also determined in the same way. It is 72%, significantly larger than that in the 1 mol/kg $LiBF_4$ solution. This is consistent with many previous results supporting that $LiPF_6$ has a larger dissociation constant than $LiBF_4$ in many organic solvents.[1]

It is interesting to compare our results to those in a recent paper based on Raman measurements.[11] In the work, the authors assumed the transition moments of Li^+-bound and unbound acetonitrile molecules to be the same and did not take into consideration that the neutral ion pairs may not change the CN stretch frequency. They determined the coordination number of Li^+ in the 1 M $LiBF_4$ acetonitrile solution to be 2.1. The Li^+ coordination number is obviously underestimated by the method because of the two reasons mentioned. The same group also published a paper regarding the coordination number of Li^+ in a $LiPF_6$/acetonitrile crystal determined with XRD.[10] In the crystal, one Li^+ is surrounded by six acetonitrile molecules of which four are very close to Li^+ and the other two are lightly farther away from the cation. In other words, the coordination number is between 4 and 6, dependent on how the coordination number is defined. From our experimental results, the coordination number is also 4−6. The two results from solutions and crystals are amazingly close. The reason for such a similarity is probably because the binding of Li^+ with CH_3CN is so strong that the energy change during the phase transition from liquid to solid is not sufficient to alter the ion/solvent complex structure.

4. CONCLUDING REMARKS

In this work, we show that the Li^+ coordination number in acetonitrile solutions can be determined by directly measuring the rotational times of solvent molecules bound and unbound to it. We find that regardless of the nature of the anions and the concentrations (from 0.2 to 2 M), the Li^+ coordination number is 4−6. However, the dissociation constants of the salt are dependent on the nature of the anions. We determine that in 1 M $LiBF_4$ solution, 53% of the salt dissociates into Li^+, which is bound by 4−6 solvent molecules. In 1 M $LiPF_6$ solution, 72% of the salt dissociates. 2D IR experiments also show that the binding between Li^+ and acetonitrile is very strong. The lifetime of the complex is much longer than 19 ps. According to our previous studies,[27,28] the formation enthalpy absolute value of the Li^+/acetonitrile complex is estimated to be larger than 3 kcal/mol.

In principle, the method demonstrated here is applicable to determine the Li^+ coordination numbers in other Li^+ nonaqueous solutions, e.g., esters, as the Li^+-bound and unbound ester molecules have different C═O stretch and C—O stretch frequencies. However, the relatively short vibrational lifetimes of these two probes require extra efforts to extract the molecular rotational times out of the severely heat-contaminated signals.

■ ASSOCIATED CONTENT

Supporting Information

Figures and tables about the anisotropy decay and relative viscosities of various samples. The material is available free of charge via the Internet at http://pubs.acs.org.

■ AUTHOR INFORMATION

Corresponding Author

*J. Zheng: e-mail, junrong@rice.edu.

Notes

The authors declare no competing financial interest.

■ ACKNOWLEDGMENTS

This work is supported by the National Natural Science Foundation of China (No. 21373213), the Chinese Academy of Sciences, and the Ministry of Science and Technology. J.R.Z. is supported by the Welch foundation under Award No. C-1752, the Air Force Office of Scientific Research under AFOSR Award No. FA9550-11-1-0070., and the David and Lucile Packard Foundation. We also appreciated Thomas Nguyen at Rice for his viscosity measurements. Insightful discussions from Deen Jiang at Oakridge national lab are highly appreciated.

■ REFERENCES

(1) Xu, K. Nonaqueous Liquid Electrolytes for Lithium-based Rechargeable Batteries. *Chem. Rev.* **2004**, *104*, 4303−4417.
(2) Kim, Y.; Goodenough, J. B. Challenges for Rechargeable Li Batteries. *Chem. Mater.* **2010**, *22*, 587−603.
(3) Besenhard, J. O.; Winter, M.; Yang, J.; Biberacher, W. Filming Mechanism of Lithium-Carbon Anodes in Organic and Inorganic Electrolytes. *J. Power Sources* **1995**, *54*, 228−231.
(4) Bogle, X.; Vazquez, R.; Greenbaum, S.; Cresce, A. V. W.; Xu, K. Understanding Li^+−Solvent Interaction in Nonaqueous Carbonate Electrolytes with ^{17}O NMR. *J. Phys. Chem. Lett.* **2013**, *4*, 1664−1668.
(5) Xu, K.; Lam, Y.; Zhang, S.; Jow, T. R.; Curtis, T. Solvation Sheath of Li^+ in Non-Aqueous Electrolytes and Its Implication of Graphite/Electrolyte Interface Chemistry. *J. Phys. Chem. C* **2007**, *111*, 7411−7421.
(6) Xu, K. Charge-Transfer Process at Graphitic Anode/Electrolyte Interface and Solvation Sheath Structure of Li^+ in Non-aqueous Electrolytes. *J. Electrochem. Soc.* **2007**, *154*, 162−167.
(7) Blint, R. J. Binding of Ether and Carbonyl Oxygens to Lithium Ion. *J. Electrochem. Soc.* **1995**, *142*, 696−702.
(8) Ogara, J. F.; Nazri, G.; Macarthur, D. M. A C^{13} and Li^6 Nuclear-Magnetic- Resonance Study of Lithium Perchlorate Poly (Ethylene-Oxide) Electrolytes. *Solid State Ionics* **1991**, *47*, 87−96.
(9) Fukushima, T.; Matsuda, Y.; Hashimoto, H.; Arakawa, R. Solvation of lithium ions in organic electrolytes of primary lithium batteries by electrospray ionization-mass spectroscopy. *J. Power Sources* **2002**, *110*, 34−37.
(10) Seo, D. M.; Boyle, P. D.; Borodin, O.; Henderson, W. A. Li^+ cation coordination by acetonitrile-insights from crystallography. *RSC Adv.* **2012**, *2*, 8014−8019.
(11) Seo, D. M.; Borodin, O.; Han, S. D.; Boyle, P. D.; Henderson, W. A. Electrolyte Solvation and Ionic Association II. Acetonitrile-Lithium Salt Mixtures: Highly Dissociated Salts. *J. Electrochem. Soc.* **2012**, *159*, A1489−A1500.
(12) Einstein, A. *Investigations on the Theory of the Brownian Motion*; Dover: New York, 1956.
(13) Chen, H. L.; Bian, H. T.; Li, J. B.; Wen, X. W.; Zheng, J. R. Relative Intermolecular Orientation Probed via Molecular Heat Transport. *J. Phys. Chem. A* **2013**, *117*, 6052−6065.
(14) Dai, J. M.; Karpowicz, N.; Zhang, X. C. Coherent Polarization Control of Terahertz Waves Generated from Two-Color Laser-Induced Gas Plasma. *Phys. Rev. Lett.* **2009**, *103*, 023001.
(15) Dai, J.; Xie, X.; Zhang, X. C. Detection of broadband terahertz waves with a laser-induced plasma in gases. *Phys. Rev. Lett.* **2006**, *97*, 103903.
(16) Xie, X.; Dai, J. M.; Zhang, X. C. Coherent Control of THz Wave Generation in Ambient Air. *Phys. Rev. Lett.* **2006**, *96*, 75005.
(17) Bian, H. T.; Li, J. B.; Wen, X. W.; Zheng, J. R. Mode-specific Intermolecular Vibrational Energy Transfer. I. Phenyl Selenocyanate and Deuterated Chloroform Mixture. *J. Chem. Phys.* **2010**, *132*, 184505.
(18) Krief, A.; Delmotte, C.; Dumont, W. Chemoselective Reduction of Organo- Selenocyanates to Diselenides and Selenolates. *Tetrahedron* **1997**, *53*, 12147−12158.
(19) Loring, J. S.; Fawcett, W. R. Ion-Solvent Interaction in Acetonitrile Solutions of Lithium, Sodium, and Tetraethylammonium Perchlorate Using Attenuated Total Reflectance FTIR Spectroscopy. *J. Phys. Chem. A* **1999**, *103*, 3608−3617.
(20) Lakowicz, J. *Principles of Fluorescence Spectroscopy*, 3rd ed.; Springer: Berlin, 2006; p 980.
(21) Bian, H. T.; Wen, X. W.; Li, J. B.; Chen, H. L.; Han, S. Z.; Sun, X. Q.; Song, J. A.; Zhuang, W.; Zheng, J. R. Ion Clustering in Aqueous Solutions Probed with Vibrational Energy Transfer. *Proc. Natl. Acad. Sci. U. S. A.* **2011**, *108*, 4737−4742.
(22) Bian, H. T.; Chen, H. L.; Li, J. B.; Wen, X. W.; Zheng, J. R. Nonresonant and Resonant Mode-specific Intermolecular Vibrational Energy Transfers in Electrolyte Aqueous Solutions. *J. Phys. Chem. A* **2011**, *115*, 11657−11664.
(23) Woutersen, S.; Bakker, H. J. Resonant Intermolecular Transfer of Vibrational Energy in Liquid Water. *Nature* **1999**, *402*, 507−509.
(24) Bian, H. T.; Wen, X. W.; Li, J. B.; Zheng, J. R. Mode-specific Intermolecular Vibrational Energy Transfer. II. Deuterated Water and Potassium Selenocyanate Mixture. *J. Chem. Phys.* **2010**, *133*, 034505.
(25) Bian, H. T.; Li, J. B.; Zhang, Q.; Chen, H. L.; Zhuang, W.; Gao, Y. Q.; Zheng, J. R. Ion Segregation in Aqueous Solutions. *J. Phys. Chem. B* **2012**, *116*, 14426−14432.
(26) Zheng, J.; Kwak, K.; Asbury, J. B.; Chen, X.; Piletic, I.; Fayer, M. D. Ultrafast Dynamics of Solute-Solvent Complexation Observed at Thermal Equilibrium in Real Time. *Science* **2005**, *309*, 1338−1343.
(27) Zheng, J.; Fayer, M. D. Solute-Solvent Complex Kinetics and Thermodynamics Probed by 2D-IR Vibrational Echo Chemical Exchange Spectroscopy. *J. Phys. Chem. B* **2008**, *112*, 10221−10227.
(28) Zheng, J. R.; Fayer, M. D. Hydrogen Bond Lifetimes and Energetics for Solute/Solvent Complexes Studied with 2D-IR Vibrational Echo Spectroscopy. *J. Am. Chem. Soc.* **2007**, *129*, 4328−4335.
(29) Zheng, J.; Kwak, K.; Chen, X.; Asbury, J. B.; Fayer, M. D. Formation and Dissociation of Intra-intermolecular Hydrogen Bonded Solute-Solvent Complexes: Chemical Exchange 2D IR Vibrational Echo Spectroscopy. *J. Am. Chem. Soc.* **2006**, *128*, 2977−2987.
(30) Zheng, J.; Kwak, K.; Asbury, J. B.; Chen, X.; Piletic, I.; Fayer, M. D. Ultrafast Dynamics of Solute-Solvent Complexation Observed at Thermal Equilibrium in Real Time. *Science* **2005**, *309*, 1338−1343.
(31) Zheng, J.; Fayer, M. D. Solute-Solvent Complex Kinetics and Thermodynamics Probed by 2D-IR Vibrational Echo Chemical Exchange Spectroscopy. *J. Phys. Chem. B.* **2008**, *112*, 10221−10227.
(32) Zheng, J. R.; Fayer, M. D. Hydrogen Bond Lifetimes and Energetics for Solute/Solvent Complexes Studied with 2D-IR Vibrational Echo Spectroscopy. *J. Am. Chem. Soc.* **2007**, *129*, 4328−4335.
(33) Zheng, J.; Kwak, K.; Chen, X.; Asbury, J. B.; Fayer, M. D. Formation and Dissociation of Intra-intermolecular Hydrogen Bonded Solute-Solvent Complexes: Chemical Exchange 2D IR Vibrational Echo Spectroscopy. *J. Am. Chem. Soc.* **2006**, *128*, 2977−2987.
(34) Naraharisetty, S. R. G.; Kasyanenko, V. M.; Rubtsov, I. V. Bond Connectivity Measured via Relaxation-assisted Two-dimensional Infrared Spectroscopy. *J. Chem. Phys.* **2008**, *128*, 104502.
(35) Bian, H. T.; Zhao, W.; Zheng, J. R. Intermolecular Vibrational Energy Exchange Directly Probed with Ultrafast Two Dimensional Infrared Spectroscopy. *J. Chem. Phys.* **2009**, *131*, 124501.
(36) Chen, H. L.; Bian, H. T.; Li, J. B.; Wen, X. W.; Zheng, J. R. Ultrafast Multiple-mode Multiple-dimensional Vibrational Spectroscopy. *Inter. Rev. Phys. Chem.* **2012**, *31*, 469−565.
(37) Zhang, Q.; Xie, W. J.; Bian, H. T.; Gao, Y. Q.; Zheng, J. R.; Zhuang, W. Microscopic Origin of the Deviation from Stokes-Einstein Behavior Observed in Dynamics of the KSCN Aquesous Solutions: A MD Simulation Study. *J. Phys. Chem. B* **2013**, *117*, 2992−3004.